Journal of Thermal Analysis and Calorimetry, Vol. 94 (2008) 1, 281–288

NEW IMMOBILIZED SCHIFF BASES
Synthesis, complexation, characterization and thermal behaviors

E. İspir[1]* *and S. Serin*[2]

[1]Kahramanmaraş Sütçü İmam University, Faculty of Science and Arts, Department of Chemistry, Kahramanmaraş 46050, Turkey
[2]Çukurova University, Faculty of Science and Arts, Department of Chemistry, Adana 01330, Turkey

In this study, three new immobilized Schiff bases and their Co(II), Cu(II) and Ni(II) metal complexes have been prepared. The ligands silica-Si[N-(3-propyl)2,4-dihydroxybenzaldimine] (1) H_2L, silica-Si[N-(3-propyl)4-methylsalicylaldimine-3-methoxy] (2) HL and silica-Si[N-(3-propyl)2-pyridinecarboxyaldimine] (3) L have bidentate characters. Therefore, the complexes are the mononuclear. Ligands and metal complexes were characterized by FTIR, AAS and thermoanalytical techniques. On the basis of analytical data and IR studies, a 1:1 metal to ligand stoichiometry has been suggested. TG and DTA results showed that these ligands and complexes had good thermal stability. The heat capacities of ligands were reported in the temperature range 273–363 K as no thermal anomaly was found in this temperature range.

Keywords: *immobilized, metal complexes, Schiff bases, thermal behavior*

Introduction

The Schiff base compounds constitute an important class of ligands which have been extensively studied in coordination chemistry mainly due to their facile synthesis and easily tunable steric, electronic and catalytic properties. They are also useful in constructing supramolecular structures [1–3]. The first Schiff base metal complexes were already prepared and described in the literature by Schiff in 1864 [4–6]. The characterization of Schiff bases with a N_2O_2 donor atom set has been done extensively by the scientific community, due to their relevance in biological activity and, more recently, by their applications on catalysis [7]. DTA and TG were used to study the modes of thermal decompositions as well as the composition of some divalent copper, cobalt and nickel complexes of Schiff bases [8]. The metal complexes with the Schiff base as ligands have been playing an important part in the development of inorganic chemistry as a whole [9, 10].

Since 1992, mesoporous materials have been extensively studied due to their promise for practical applications, for example catalytic, optical, electronic and so on [11]. Modified silica exhibits some advantages over modified resins such as high surface areas, high thermal and chemical stability. Salen complexes have been immobilized on silica via three different approaches [12].

Two distinct approaches of immobilization of metal catalytic centers on solid supports are well known. The first one involves the use of organic polymeric structure such as polystyrene and usually a monomer is covalently linked to the ligand used for the polymerization, and which gives a polymer with ligand sites as regular blocks. Another approach of immobilization involves the use of inorganic supports. For example, organofunctionalization of the hydroxy groups on silica or alumina surface by reacting with (3-aminopropyl)triethoxysilane has been used to anchor the ligands [13]. The success of the immobilization of functional groups on silica supports is mainly due to attachment of a silylant agent containing trialkoxysilyl groups, which are chemically reactive toward the free silanol groups disposed on the active surface [14].

Aminosilanes $[(ArNH)_2SiPh_2]$ could serve as very useful chelating ligands in this regard and may have a marked influence in the activity of the resulting complex due to the presence of silicon centers adjacent to the ligating nitrogen atoms [15].

Silanes are organofunctional hybrid organic–inorganic chemicals, historically used as coupling agents for adhesion between organic and inorganic materials, such as glass fiber-reinforced polymeric composites [16–18]. A general silane structure is $(XO)_3Si(_{CH2})_nY{\cdot}XO$, with a hydrolysable alkoxy group which can be methoxy (OCH_3), ethoxy (OC_2H_5) or acetoxy ($OCOCH_3$). Y is an organofunctional group such as vinyl (C=C) or amino (NH_2) which is responsible for a good paint adhesion of a silane-treated metal surface [19]. Chemically bonded stationary phases containing amino groups in their structure are

---

* Author for correspondence: esinispir@ksu.edu.tr

1388–6150/$20.00

Akadémiai Kiadó, Budapest, Hungary
Springer, Dordrecht, The Netherlands

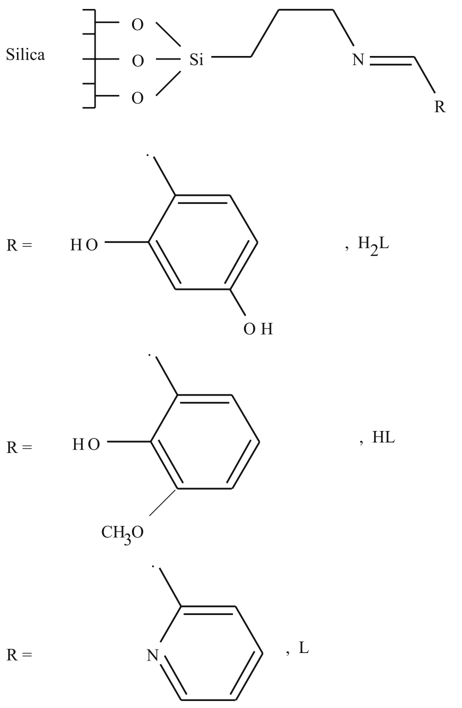

Fig. 1 The proposed structure of immobilized Schiff base ligands

known since the 1970s. Haken *et al.* [20–23] were one of the first groups to prepare and test them. They concluded that polysiloxanes with an ethylenediamine moiety with both primary and secondary amino groups in their structure can be used to effectively extract aldehydes, lactones and most ketones by chemical reactions with carbonyl compounds through the formation of carbon-nitrogen double bonds. The strong interactions also occur in the case of alcohols [24].

This article describes the syntheses, characterization and thermal properties of silica-Si[N-(3-propyl)2,4-dihydroxybenzaldimine] (1) H_2L, silica-Si[N-(3-propyl)4-methylsalicylaldimine 3-methoxy] (2) HL and silica-Si[N-(3-propyl)2-pyridinecarboxyaldimine] (3) L and their three transition metal complexes (Fig. 2). The ligands in this study were synthesized by the reaction of 2,4-dihydroxybenzaldehyde, *o*-vanillin and 2-pyridinecarboxaldehyde with immobilized 3-aminopropyltrimethoxysilane, respectively (Fig. 1). The analytical data shows that the metal to ligand ratio in the Schiff base complexes is 1:1.

Experimental

Materials

Synthesis of 3-aminopropylsilica

A sample of 20 g of activated silica gel (Kiesegel 60) was suspended in 100 mL of dry toluene and 20 mL of 3-aminopropyltrimethoxysilane (Fluka) was added to this suspension. The mixture was refluxed for 72 h. The suspension filtered and the solid was washed with water. The product was named aminopropyl silica (AMPS) and dried in air at 95°C [25].

Synthesis of silica-Si[N-(3-propyl)2,4-dihydroxy-benzaldimine] L^1H (1)

The oven dried aminopropyl silica (5 g) was added to absolute ethanol (100 mL) in a 250 round bottomed flask followed by 2,4-dihydroxybenzaldehyde (Fluka) (0.69 g, 5 mmol). The reaction mixture was stirred at 60°C for 24 h. The ligand grafted silica was filtered at the reaction temperature and washed with ethanol thoroughly to remove unreacted 2,4-dihydroxybenzaldehyde. The pale orange product was dried in air at 95°C overnight. Yield: 2.22 g, *m.p.*: >250°C (dec.).

Synthesis of silica-Si[N-(3-propyl)4-methylsalicyl-aldimine] L^2H (2)

o-Vanillin (Fluka) (0.76 g, 5 mmol) dissolved in EtOH (10 mL) was carefully added with stirring to a suspension of AMPS (5 g) in EtOH (100 mL). The bright yellow resulting mixture was allowed to stir magnetically under reflux for 24 h. The resulting precipitate was filtered, washed with cold EtOH dried in air. Yield: 2.53 g , *m.p.*: >250°C (dec.).

Synthesis of silica-Si[N-(3-propyl)2-pyridine-carboxyaldimine] L^3H (2)

2-Pyridinecarboxaldehyde (Fluka) (0.54 g, 5 mmol) and the 100 mL suspension of AMPS (5 g) were stirred until a beige precipitate appeared. Stirring was continued for 24 h and then the yellow powder was collected by vacuum filtration and dried overnight in air. Yield: 2.73 g, *m.p.*: >250°C (dec.).

Synthesis of the metal complexes

The Co(II), Cu(II) and Ni(II) complexes of immobilized Schiff base ligands were prepared according to method [26].

The complexes were prepared by stirring mixture of appropriate ligand-grafted silica (Schiff base) (4 g) and metal acetates [$Co(AcO)_2\cdot 4H_2O$, $Cu(AcO)_2\cdot H_2O$ and $Ni(AcO)_2\cdot 4H_2O$)] (Merck) (0.5 mmol) in acetone (100 mL) at room temperature for 24 h. After stirring, complexes were filtered, washed with acetone till washings were colorless. They were dried in air at 95°C overnight and then conditioned for a total of 27 h (3×3 each refluxing in toluene and ethanol). The complexes were dried at 70°C in a vacuum oven for

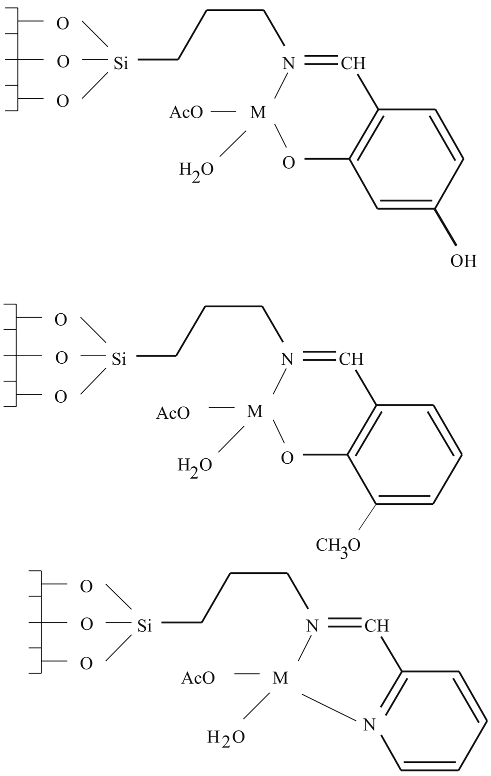

Fig. 2 The proposed structures of the immobilized Schiff base complexes. *M*=Cu(II), Co(II) and Ni(II)

4 h before analyses. The probable structures of complexes are shown in Fig. 2.

Physical measurements

I.R. spectra of ligands and complexes were obtained using KBr discs (4000–400 cm^{-1}) on a Shimadzu 8300 FTIR spectrophotometer. Thermal analyses were performed on Perkin Elmer Diamond TG/DTA models using 10 mg samples. The DTA and TG curves were obtained at a heating rate of 10°C min^{-1} in dry N_2 atmosphere in the 0–1110°C range. The heat capacity values were carried out with a Perkin Elmer Sapphire DSC, in nitrogen using Al. The atomic absorption analyses were performed on A.A. Analyst 800-Perkin Elmer model. Samples (0.05 g) were dissolved HNO_3 (2%, 5 mL) prior to analysis.

Result and discussion

In this study, silica-Si[N-(3-propyl)2,4-dihydroxy-benzaldimine] (1) H_2L, silica-Si[N-(3-propyl)4-methyl-salicylaldimine] (2) HL and silica- Si[N-(3-propyl)2-pyridinecarboxyaldimine] (3) L Schiff base ligands were prepared by the reaction of 2,4-dihydroxy-benz-aldehyde, *o*-vanillin and 2-pyridine-carboxaldehyde with 3-aminopropyl-trimethoxy-silane. The complexes were synthesized by the general equations shown below. In ethanolic solution, the ligand undergoes deprotonation to form 1:1 mononuclear metal chelates with some transition metal ions.

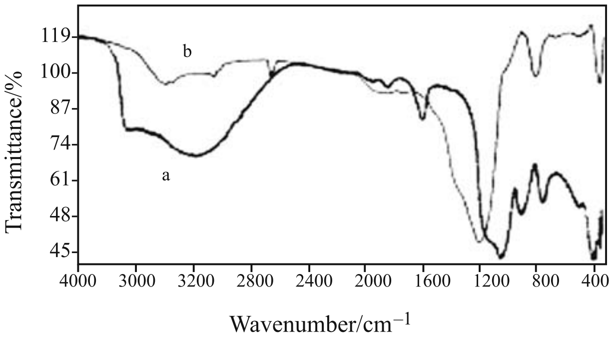

Fig. 3 The IR spectra of a – silica gel and b – aminopropyl silica (AMPS)

The Schiff base ligands were synthesized in good yields in toluene. The ligands and the complexes are stable at room temperature. The probable structures of complexes were shown in Fig. 2.

The IR spectra of the ligands and their complexes have been studied in order to characterize their structures. The characteristic IR data of the Schiff Base ligands and their metal complexes listed in Table 1.

The IR spectra of pure silica gel (a) and synthesized compound aminopropyl silica (AMPS) (b) are shown in Fig. 3. In this spectra, the silica gel (a) shows the broad band in the range 3430–3080 cm^{-1} can be attributed to the silanol OH groups and the broad absorption at 1089 cm^{-1} is attributed to Si–O–Si bonds in silica [13, 27]. When the silica gel reacts with 3-aminopropyltrimethoxysilane, the compound AMPS occur. In this compounds spectra, the band at 3350 cm^{-1} may be assigned to the $\nu(NH_2)$ vibration. The weak bands at the range 2924–2856 cm^{-1} can be attributed to the aliphatic ν_{CH2} groups.

The IR spectra of H_2L (a), HL (b) and L (c) are shown in Fig. 4. Immobilized Schiff base ligands

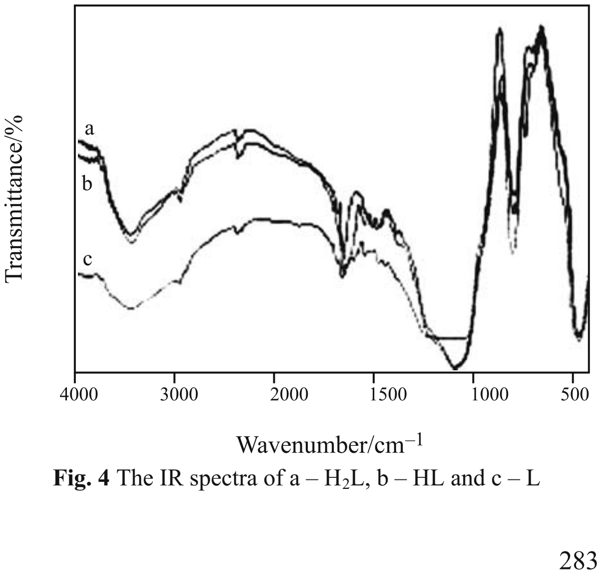

Fig. 4 The IR spectra of a – H_2L, b – HL and c – L

synthesized with AMPS and carbonyl compounds. In their spectrums, the vibration of NH_2 at 3350 cm^{-1} is disappeared. Instead of this band, a new strong band formed at between of 1650–1625 cm^{-1}. These bands are due to C=N stretching frequencies [11]. The bands in between 1648–1635 cm^{-1} in the spectra (Fig. 4) show that carbonyl groups react with AMPS successfully [28]. In the spectra of the immobilized ligands, a strong broad absorptions in the range 3450–3443 cm^{-1} show the silanol OH and free OH stretching non participation of phenolic OH group in coordination [13, 29]. The IR spectra of the ligands and complexes show characteristic bands in the range 3062–3035 cm^{-1}, which are not observed in the IR spectra of AMPS. These bands are belong to aromatic C–H bands for ligands and complexes [10]. The IR spectrum of 3-aminopropyl silica displays characteristic aliphatic C–H stretching bands in the range ~2940 and ~286 cm^{-1} [26, 30]. Schiff base ligands show characteristic vibrations at around 1092 and 910 cm^{-1} corresponding to the stretching vibrations of Si–O–Si bands, respectively [13, 31].

The IR spectra of immobilized Schiff base complexes are similar. The IR spectral data are given in Table 1. In the IR spectra of the complexes that derived H_2L shows a band around 3410 cm^{-1}, which can be attributed to the free OH stretching mode indicating non-participation of OH group in coordination [32]. Metal complexes show significant differences from ligands. After coordination between immobilized Schiff base ligands and Co(II), Cu(II) and Ni(II) metal salts, the C=N stretching frequencies slightly shift to lower wave number region [11]. The lowering in frequencies of the C=N peak is indicative of the formation of metal–ligand bonds [26]. Immobilized Schiff base ligands, without metal, showed the C=N absorption at ~1640 cm^{-1}, and a decrease of ~20 cm^{-1} in $\nu_{C=N}$ is seen due to the complexation with cobalt [13, 26]. Aromatic ring C–H absorptions are observed at 3035 cm^{-1}.

Table 2 Summary of AAS data for the immobilized Schiff base complexes

Compound	Total reaction time/h	Nominal loading of metal/ mmol g^{-1}	Metal analysis (AAS)/ mmol g^{-1}
$[Co(H_2L)(OAc)(H_2O)]$	24	0.125	0.049
$[Cu(H_2L)(OAc)(H_2O)]$	24	0.125	0.76
$[Ni(H_2L)(OAc)(H_2O)]$	24	0.125	0.34
$[Co(HL)(OAc)(H_2O)]$	24	0.125	0.011
$[Cu(HL)(OAc)(H_2O)]$	24	0.125	0.08
$[Ni(HL)(OAc)(H_2O)]$	24	0.125	0.068
$[Co(L)(OAc)(H_2O)]$	24	0.125	0.04
$[Cu(L)(OAc)(H_2O)]$	24	0.125	0.026
$[Ni(L)(OAc)(H_2O)]$	24	0.125	0.069

For the metal complexes, new weak bands in the 611–594 and 445–418 cm^{-1} range may be attributed to ν_{M-O} and ν_{M-N} [33], respectively.

The metal loadings determined by AAS are summarized in Table 2, according to the literature [33]. The reaction time is stable for all complexes. The data show that we succeed in complexation with metal acetates and ligands. Quantity of loading metals and the AAS data of metals confirm that ligand-metal ratio is 1:1 for all complexes.

Thermal behaviors of ligands and metal complexes have been studied using thermogravimetric analysis (TG) and differential thermal analysis (DTA) equipments. The curves which belong to ligands are present in Fig. 5. The temperature ranges, mass loss

Table 1 Characteristic IR bands of the Schiff base ligands and their metal complexes/cm^{-1}, KBr

Compound	ν_{OH}	ν_{ArC-H}	$\nu_{aliph.C-H}$	$\nu_{CH=N}$	ν_{Si-O}	ν_{M-N}	ν_{M-O}
H_2L	3445	3058	2941–2849	1648	1095	–	–
$[Co(H_2L)(OAc)(H_2O]$	3410	3057	2941–2855	1622	1027	596	422
$[Cu(H_2L)(OAc)(H_2O]$	3412	3038	2941–2849	1608	1030	599	418
$[Ni(H_2L)(OAc)(H_2O]$	3409	3057	2942–2856	1612	1031	563	445
HL	3450	3055	2931–2883	1643	1047	–	–
$[Co(HL)(OAc)(H_2O]$	3416	3058	2939–2865	1616	1036	607	418
$[Cu(HL)(OAc)(H_2O]$	3412	3062	2940–2855	1606	1039	594	420
$[Ni(HL)(OAc)(H_2O]$	3419	3057	2940–2862	1618	1042	611	420
HL	3443	3057	2940–2862	1645	1097	–	–
$[Co(L)(OAc)(H_2O]$	3423	3055	2935–2853	1625	1056	605	417
$[Cu(L)(OAc)(H_2O]$	3429	3035	2929–2845	1610	1087	596	438
$[Ni(L)(OAc)(H_2O]$	3405	3052	2930–2839	1618	1089	601	420

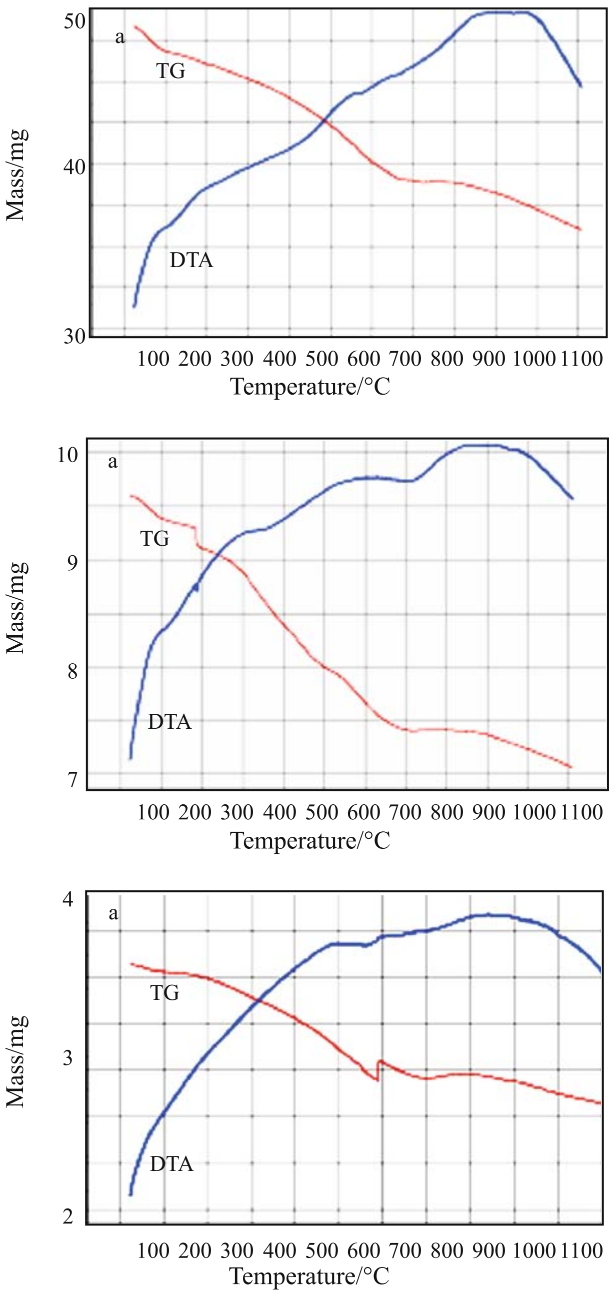

Fig. 5 TG and DTA of a – H_2L, b – HL and c – L

Table 3 Thermal properties of immobilized Schiff base ligands

Immobilized Schiff base ligands	T_d^a/°C	$W^b_{ava.}$/mg s^{-1}	Residue/%	Mass loss/%
H_2L	228.17	0.023	74.95	25.05
HL	215.52	0.043	76.50	24.40
L	283.80	0.016	76.34	23.66

[a] Experimental results from TG (5% decomposition)
[b] Available reaction speed

percentages of ligands are given in Table 3. The results show that the immobilized ligands generally decompose in several thermal events, i.e., three or four decomposition steps. The characteristic mass losses related to water were detected between 50–110°C for all curves. After this common step all ligands showed a decomposition stage [8]. The main mass losses in the temperature range of 400–700°C corresponds to the splitting of the Schiff base molecules coupled to the activated silica [14]. The final peaks in the region of 700–1100°C due to partly thermal decompositions of the silica structure [29]. The ligand L has the higher decomposition temperature for 5% mass losses. Three ligands % residues and % mass losses are similar.

Differential scanning calorimetry (DSC) was performed at a heating rate of 10°C min^{-1} under nitrogen atmosphere. From the DSC experiments (Table 5), the results indicate that the ligands had a higher T_g, because of the intimate mixing of the organic and inorganic components in the final materials. With increasing silica contents, the higher silica content results in a greater number of polymer silicate bonds and more restriction of the polymer chain movement resulting in the higher T_g value.

Thermal behaviors of complexes have been studied using TG and DTA. Thermogravimetric data of complexes are given in Table 4. Thermal curves obtained for most of the complexes were very similar in character. The curve of [Cu(HL)(OAc)(H_2O)] is taken as a represantive example and shown in Fig. 6. All complexes shows a mass loss of 5%, which is appeared below 280°C.

The TG curves of [M(L)(OAc)(H_2O)] consist mainly of three steps in the range 23–150, 150–700 and 700–1100°C. The first estimated mass losses (%) for [M(L)(OAc)(H_2O)] are of 1.16, 11.46, 10.23, 9.67, 10.23, 9.75, 11.65, 11.86 and 11.47 within the temperature range of 23–150°C may be attributed to the losses of solvent and coordinated water molecules [13]. Some decomposition could be correlated

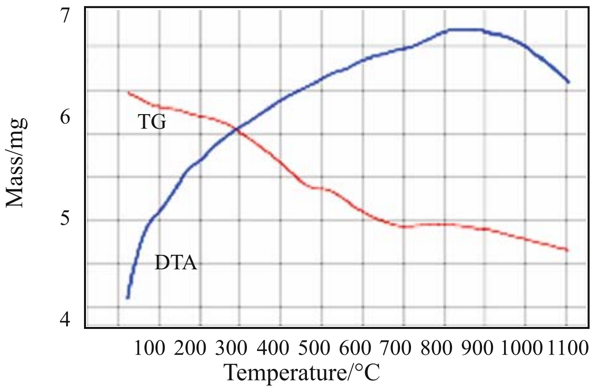

Fig 6 TG and DTA of [Cu(HL)(OAc)(H_2O)]

Table 4 Thermogravimetric data of complexes

Metal complexes	TG range/°C	Mass loss/%	Assignment
$[Co(H_2L)(OAc)(H_2O)]$	23–150	10.16	solvent and water evolution
	150–700	76.76	decomp. of ligand and formation metal oxide
$[Cu(H_2L)(OAc)(H_2O)]$	23–150	11.46	solvent and water evolution
	150–700	76.23	decomp. of ligand and formation metal oxide
$[Ni(H_2L)(OAc)(H_2O)]$	23–150	10.23	solvent and water evolution
	150–700	78.57	decomp. of ligand and formation metal oxide
$[Co(HL)(OAc)(H_2O)]$	23–150	9.67	solvent and water evolution
	150–700	75.89	decomp. of ligand and formation metal oxide
$[Cu(HL)(OAc)(H_2O)]$	23–150	10.23	solvent and water evolution
	150–700	75.16	decomp. of ligand and formation metal oxide
$[Ni(HL)(OAc)(H_2O)]$	23–150	9.75	solvent and water evolution
	150–700	77.59	decomp. of ligand and formation metal oxide
$[Co(L)(OAc)(H_2O)]$	23–150	11.65	solvent and water evolution
	150–700	79.82	decomp. of ligand and formation metal oxide
$[Cu(L)(OAc)(H_2O)]$	23–150	11.86	solvent and water evolution
	150–700	79.13	decomp. of ligand and formation metal oxide
$[Ni(L)(OAc)(H_2O)]$	23–150	11.47	solvent and water evolution
	150–700	78.36	decomp. of ligand and formation metal oxide

with the proper decomposition products. The decomposition of all complexes in air ended with silica and metal oxide formation. The next estimated mass losses (%) for $[M(L)(OAc)(H_2O)]$ are of 76.76, 76.23, 78.57, 75.89, 75.16, 77.59, 79.82, 79.13 and 78.36 within the temperature range of 150–700°C may be attributed to the losses of ligand molecule and formation of metal oxides [34, 35]. The $[Cu(HL)(OAc)(H_2O)]$ shows a mass loss of 5%, which is appeared at 269.4°C. However, for the corresponding supported complex, there is a continuous mass loss, which extends above 1104°C. Therefore, these features confirmed the thermal stability of complex.

The heat capacity is a characteristic material property [36]. Heat capacity values were measured DSC Sapphire, in nitrogen using Al, crucibles and lids. The baseline was obtained by running with empty crucibles or with crucibles containing a standard material (Sapphire) under the same measurement conditions used for the sample substance (atmosphere in the measuring cell, flow rate for operation with dynamic gas, initial temperature, heating rate and scanning rate (sampling interval), mass of crucible and lid and position of crucible in the cell). The entire temperature ranged over, which the C_p curve was to be determined, could be continuously scanned in a heating phase. The entire measuring system must be at a uniform, stable temperature level. To equalize the temperature in the system, a constant temperature segment prior to starting the heating phase was defined.

After the run of the three measurements (baseline, standard calibration material Sapphire as baseline+correction, sample also as baseline+correction), individual C_p values at different temperatures were determined according to the following equation:

$$C_p = \frac{m_{\text{standard}}}{m_{\text{sample}}} \frac{\text{DSC}_{\text{sample}} - \text{DSC}_{\text{bas}}}{\text{DSC}_{\text{standard}} - \text{DSC}_{\text{bas}}} C_{\text{p. standard}}$$

C_p: heat capacity of the sample at temperature T, J K^{-1} g^{-1}; $C_{\text{p.standart}}$: heat capacity of the standard at temperature at temperature T, J K^{-1} g^{-1}; m_{standard}: mass of the standard, mg; m_{sample}: mass of the sample, mg; $\text{DSC}_{\text{standard}}$: value of the DSC signal at temperature T from the standard curve μV; $\text{DSC}_{\text{sample}}$: value of the DSC signal at temperature T from the sample curve μV; DSC_{bas}: value of DSC signal at temperature T from the baseline curve, μV.

The aim of the DSC measurements is to investigate the relation between heat capacity and temperature. The experiments were carried out to determine the heat capacities of the samples in the temperature range 273 to 363 K. The data of C_p are listed in Table 5. No thermal abnormality was found in this temperature range. The heat capacities of the ligands tend to increase with the increase of the temperature.

Table 5 Experimental data of heat capacities of ligands

	C_p/J K^{-1} g^{-1}				C_p/J K^{-1} g^{-1}		
T/K	H_2L	HL	L	*T*/K	H_2L	HL	L
273.15	0.884	0.820	1.735	275.15	0.929	0.841	1.775
277.15	0.957	0.868	1.782	279.15	0.975	0.891	1.791
281.15	1.017	0.912	1.814	283.15	1.041	0.933	1.827
285.15	1.076	0.955	1.907	287.15	1.105	0.976	1.913
289.15	1.139	1.001	1.922	291.15	1.185	1.023	1.930
293.15	1.211	1.043	1.942	295.15	1.222	1.064	1.953
297.15	1.258	1.081	1.960	299.15	1.279	1.096	1.966
301.15	1.300	1.110	1.971	303.15	1.319	1.119	1.979
305.15	1.345	1.127	1.985	307.15	1.380	1.132	1.991
309.15	1.387	1.135	2.081	311.15	1.406	1.146	2.152
313.15	1.429	1.162	2.095	315.15	1.453	1.179	2.081
317.15	1.483	1.193	2.092	319.15	1.512	1.211	2.106
321.15	1.543	1.228	2.121	323.15	1.575	1.237	2.201
325.15	1.604	1.253	2.204	327.15	1.631	1.271	2.210
329.15	1.656	1.296	2.210	331.15	1.676	1.301	2.228
333.15	1.693	1.326	2.242	335.15	1.707	1.348	2.261
337.15	1.718	1.365	2.277	339.15	1.724	1.384	2.299
341.15	1.729	1.391	2.316	343.15	1.728	1.415	2.339
345.15	1.722	1.428	2.357	347.15	1.713	1.447	2.375
349.15	1.703	1.463	2.400	351.15	1.694	1.479	2.416
353.15	1.715	1.513	2.446	355.15	1.726	1.538	2.455
357.15	1.766	1.552	2.470	359.15	1.783	1.574	2.488
361.15	1.809	1.591	2.503				

Conclusions

Three new immobilized Schiff base and their Co(II), Cu(II) and Ni(II) metal complexes were synthesized. Ligands and metal complexes were characterized by Fourier Transform Infrared spectroscopy, Atomic Absorption spectroscopy and Thermal Analyses. TG and DTA results showed that these ligands and complexes had good thermal stability. The heat capacities of ligands were reported for the temperature range 273 and 363 K as no thermal abnormality was found in this temperature range.

Acknowledgements

The author thanks Barış Avar and Musa Göğebakan, Physics Department, Faculty of Science and Arts, Kahramanmaraş Sütçü İmam University, Kahramanmaraş, Turkey for the thermal analyses mesurements.

References

1 S. J. Lippard and J. M. Berg, Principles of Bioinorganic Chemistry, University Science Books, California 1994.

2 D. E. Fenton, Bioinorganic Chemistry, Oxford University Press, Oxford 1995.

3 Y. Yoshikawa, E. Ueda, K. Kawabe, K. Miyabe, T. Takino, H. Sakurai and Y. Kojima, J. Biol. Inorg. Chem., 7 (2002) 68.

4 H. Schiff, Ann. Chem. Suppl., 3 (1864) 343.

5 H. Schiff, Ann. Chem., 150 (1869) 193.

6 H. Schiff, Ann. Chem., 151 (1869) 186.

7 M. D. M. C. Ribeiro da Silva, N. R. M. Araújo, A. L. R. Silva, L. C. M. da Silva, N. P. S. M. Barros, J. M. Gon-Alves and M. A. V. Ribeiro da Silva, J. Therm. Anal. Cal., 87 (2007) 291.

8 R. M. Issa, S. A. Amer, I. A. Mansour and A. I. Abdel-Monsef, J. Therm. Anal. Cal., 90 (2007) 261.

9 P. J. Toscano and L.G. Marzilli, Progr. Inorg. Chem., 31 (1984) 105.

10 A. Valent, M. Melník, D. Hudecová, B. Dudová, R. Kivekäs and M. R. Sundberg, Inorg. Chim. Acta, 340 (2002) 15.

11 H. Zhang, P. Zhang, K. Ye, Y. Sun, S. Jiang, Y. Wang and W. Pang, J. Luminescence, 117 (2006) 68.

12 V. Mirkhani, M. Moghadam, S. Tangestaninejad and B. Bahramian, Appl. Catal. A: General, 313 (2006) 122.

13 A. S. Amarasekara, A. R. Oki, I. Mcneal and U. Uzoezie, Catal. Commun., 8 (2007) 1132.

14 A. G. S. Prado, J. A. A. Sales and C. Airoldi, J. Therm. Anal. Cal., 70 (2002) 191.

15 R. Murugavel, N. Palanisami and R. J. Butcher, J. Organo Organomet. Chem., 675 (2003) 65.

16 E. P. Plueddemann, Silane Coupling Agents, 2nd Ed., Plenum Press, New York 1991.

17 (a) K. L. Mittal (Ed.), Silanes and Other Coupling Agents, VSP, Utrecht 1992.

18 K L. Mittal (Ed.), Silanes and Other Coupling Agents, 2, VSP, Utrecht 2000.

19 D. Zhu and W. J. V. Ooij, Electrochim. Acta, 49 (2004) 1113.

20 J. R. Ashes and J. K. Haken, J. Chromatogr., 60 (1972) 33.

21 J. R. Ashes and J. K. Haken, Anal. Chem., 45 (1973) 1131.

22 J. Appleyard and J. K. Haken, J. Chromatogr., 99 (1974) 319.

23 J. K. Haken and D. K. M. Ho, J. Chromatogr., 112 (1975) 135.

24 W. Wasiak and W. Urbaniak, J. Chromatography A, 757 (1997) 137.

25 A. G. S. Prado, B. S. Miranda, J. A. Dias, Colloids and Surfaces A: Physicochem. Eng. Aspects, 242 (2004) 137.

26 S. Paul and J. H. Clark, J. Mol. Catal. A: Chem., 215 (2004) 107.

27 M. Zaharescu, A. Jitianu, A. Brãileanu, J. Madarász , Cs. Novák and G. Pokol, J. Therm. Anal. Cal., 71 (2003) 421.

28 Y. Luo and J. Lin, Microporous Mesoporous Mater., 86 (2005) 23.

29 T. Luts, W. Suprun, D. Hofman, O. Klepel, H. Papp, J. Mol. Catal. A: Chem., 261 (2007) 16.

30 A. P. M. Alves, A. L. P. Silva, O. G. da Silva, M. G. da Fonseca, L. N. H. Arakaki and J. G. P. Espínola, J. Therm. Anal. Cal., 87 (2003) 771.

31 R. Nava, T. Halachev, R. Rodriguez and V. M. Castano, Appl. Catal. A: General, 231 (2002) 131.

32 R. Gup and B. Kýrkan, Spectrochim. Acta Part A, 64 (2006) 809.

33 U. G. Singh, R. T. Williams, K. R. Halam and G. C. Allen, J. Solid State Chem., 178 (2005) 3405.

34 S. H. Patel, P. B. Pansuriya, M. R. Chhasatia, H. M. Parekh and M. N. Patel, J. Therm. Anal. Cal., 91 (2008) 413.

35 H. M. Parekh, P. K. Panchal and M. N. Patel, J. Therm. Anal. Cal., 86 (2007) 803.

36 F. Qiu, Y. Jiang, Y. Zhou and J. Liu, Silicon Chem., 3 (2006) 65.

Received: November 29, 2007
Accepted: January 22, 2008
OnlineFirst: August 15, 2008

DOI: 10.1007/s10973-007-8900-3